Revista Mexicana de Astronomía y Astrofísica, **61**, 117–122 (2025)

https://doi.org/10.22201/ia.01851101p.2025.61.01.09

LONG-TERM VARIABILITY OF WATER MASER EMISSION IN S128

E. E. Lekht[1], J. E. Mendoza-Torres[2], N. T. Ashimbaeva[1], V. V. Krasnov[3], and V. R. Shoutenkov[4]

Received September 13 2024; accepted February 14 2025

ABSTRACT

The evolution of the H_2O maser emission at the S128 source during 1981-2024 is analyzed, based on long-term regular observations. The emission from −73 to −70 km/s corresponds mainly to source B, while that of velocities < −76 km/s to source A. It was identified that in the time interval 2004-2006, the maser activity gradually shifted from source B to source A. The active phases of masers B and A lasted approximately 23 and 16 years, respectively. It is assumed that the common cause of the variability of the maser emission at both sources (A and B) can be shock waves that occur near the ionization front. When clouds collide, a disturbance propagates along the resulting ionization front, which leads to the appearance of shock waves. It is shown that the disturbance is spreading in the south-north direction. The star formation process occurs in the same direction.

RESUMEN

Se analiza la evolución de la emisión maser de H_2O en la fuente S128 durante 1981-2024, con base en su monitoreo regular. La emisión de −73 a −70 km/s proviene principalmente de la fuente B, mientras que la de < −76 km/s de la fuente A. Se identificó que en el intervalo de tiempo 2004−2006, la actividad maser cambió gradualmente de la fuente B a la fuente A. Las fases activas de los maseres B y A duraron aproximadamente 23 y 16 años, respectivamente. Se supone que la causa común de la variabilidad de la emisión maser en ambas fuentes (A y B) puede ser ondas de choque, que ocurren cerca del frente de ionización. Cuando las nubes chocan, la perturbación se propaga a lo largo del frente de ionización resultante, que conduce a la aparición de ondas de choque. Se observa que la perturbación se está extendiendo en dirección sur−norte. El proceso de formación estelar ocurre en la misma dirección.

Key Words: clouds — masers — stars formation

1. INTRODUCTION

Maser emission sources have been found to be associated with a variety of distributions of active star formation regions. In addition to the frequent appearance of OH masers at hyper-compact H II regions, masers can be located at the front of shock waves. Such configurations can occur, for example, during the movement of the H II region in the molecular core of the interstellar medium. At high velocities, the H II region acquires a comet-like shape and a shock wave front appears at the boundary between the leading region and the interstellar medium. Favorable conditions for maser radiation arise near this front. An example of such a configuration is the star formation region W44C (G 34.3+0.15), shown in Figure 1. This hyper-compact H II region is embedded in a compact molecular core with a temperature of about 225 K and a hydrogen density of $10^7 cm^{-3}$ (Wood & Churchwell 1989)

Another possible scenario could be that of two interacting (colliding) molecular CO clouds. Favorable conditions for maser emission arise at the boundary between them. An example of such a structure is the active star formation region S128. A schematic rep-

[1]Lomonosov Moscow State University, Sternberg Astronomical Institute, Moscow, 119991 Russia.
[2]Instituto Nacional de Astrofísica, Óptica y Electrónica, Puebla, México.
[3]Lebedev Physical Institute, Astro Space Center, Russian Academy of Sciences, Moscow, 117997 Russia.
[4]Pushchino Radio Astronomy Observatory, Astro Space Center, Lebedev Physical Institute, Russian Academy of Sciences, Pushchino, 142290 Russia.

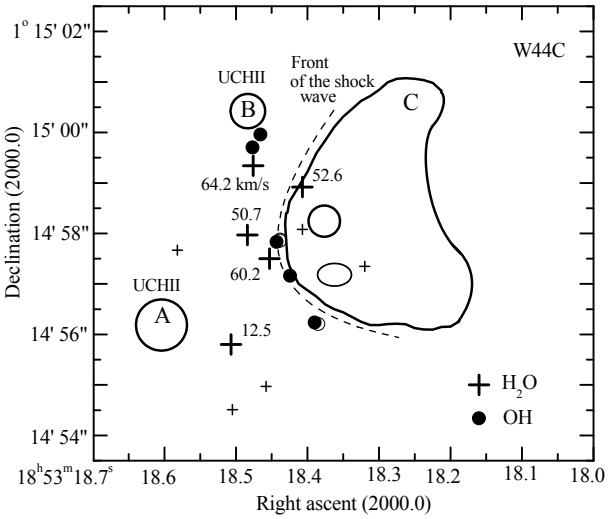

Fig. 1. The structure of the W44C star formation region. Crosses indicate the positions of clusters of H_2O maser spots. Bold crosses correspond to the main clusters, the labels near them refer to the radial velocities of the main features. The circles represent the positions of the main OH emission areas.

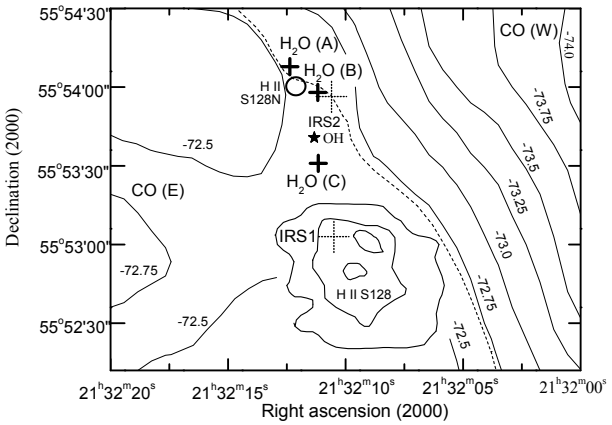

Fig. 2. The structure of the S128 star formation region. Crosses denote the locations of the H_2O maser spots, the bold ones indicate the main H_2O spot clusters, (see text).

resentation of the S128 source is shown in Figure 2. The basic data for constructing this figure were taken from Haschick & Ho (1985) and from Ashimbaeva et al. (2023).

The distance to S128 is assumed to be the kinematic one, which is equal to 7.5 kps. The CO(E) cloud of Figure 2 has a small radial velocity gradient. The CO(W) cloud has a radial velocity of −74 km/s with no velocity gradient in it. Between the clouds, the medium is highly compressed and has a large radial velocity gradient. In addition, an ionization front appears along the boundary of the cloud interaction.

It is assumed that a more distant CO cloud is pushing the collision area towards us. According to Richards et al. (2005) the disturbance spreads from south to north.

A hyper-compact region, whose size is $\approx 3''$, is located near the ionization front of the S128N H II region (Ho et al. 1981), at a distance of $60''$, on the south of the hyper-compact H II region. It is S128, an extended H II region (Ho et al. 1981). Near each H II region there is an IR source: IRS1 near the extended region, and IRS2 near the hyper-compact region H II (Mampaso et al. 1984). It is believed that the star formation process in S128 takes place along the boundary that separates the colliding clouds CO(E) and CO(W).

Along the ionization front, at the North and at the South of the H II S128N hyper-compact region, two sources of H_2O maser emission, denoted respectively, as A and B, and separated by a distance of $13''$, have been detected (Ho et al. 1981; Haschick & Ho 1985; Migenes et al. 1999). A third maser source of water vapor is located $30''$ south of S128N (Richards et al. 2005). However, unlike A and B, maser C is quite far away from the ionization front. The masers are associated with the ionization front, not with a specific young stellar object (YSO). Some clusters of maser condensations are elongated by hundreds of astronomical units.

The study of the variability of maser emission H_2O is described in the works of Berulis et al. (1995), Lekht et al. (2002) and Ashimbaeva et al. (2018).

The hydroxyl maser is also located far from the ionization front. The emission of this maser was discovered in 1986 (Wouterloot et al. 1988). It is located south of the super-compact H II region S128N. The OH maser emission is quite weak. The study of the variability of OH emission in the 18 cm line was described in the works of Ashimbaeva et al. (2018, 2023).

In this work we focus on the study of the long-term variability of H_2O maser emission in S128, during the entire period of our monitoring, which extends for more than forty years (from 1981 to 2024).

2. OBSERVATIONS AND CONSTRUCTION OF 3D IMAGES

Regular long-term observations of the H_2O maser emission in the direction of S128 ($\alpha_{2000} = 21^h32^m13^s, \delta_{2000} = 55°54'39''$) were performed at the 22-m radio telescope in Pushchino Radio Astronomy Observatory (PRAO), in Russia, from 1981 to 2024. The FWHM of the beam antenna of the radio telescope, at a wavelength of 1.35 cm, is $2.6'$. The

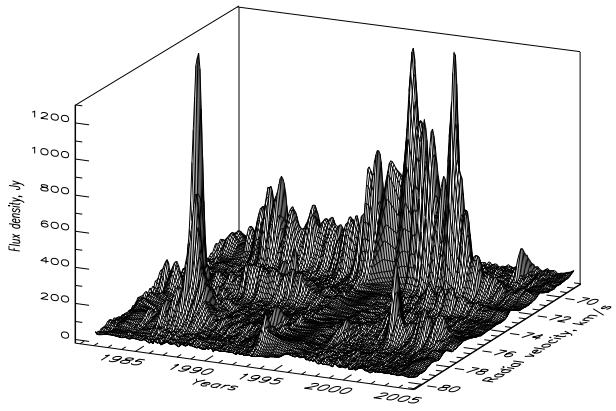

Fig. 3. 3D representation of H_2O maser emission spectra in S128 in the period 1981–2005. (see text).

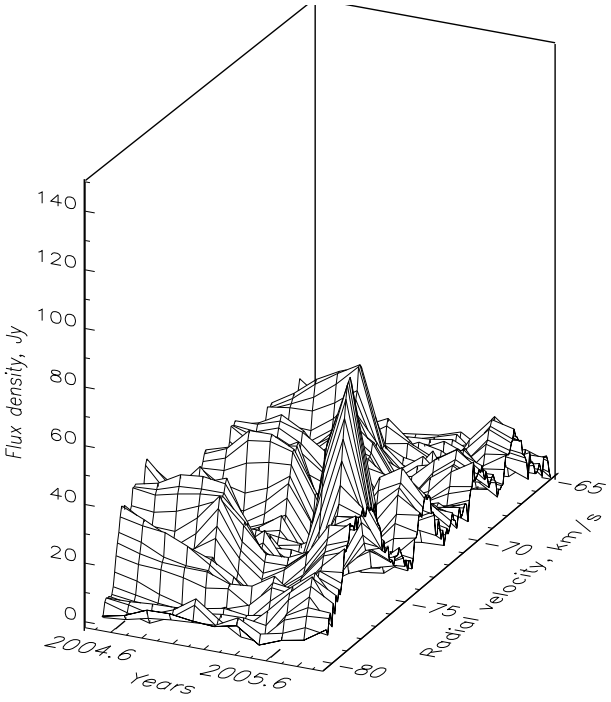

Fig. 4. 3D representation of H_2O spectra in S128 during the period 2004.5–2006 (see text).

noise temperature of the system was in the range of 150–300 K, depending on the observational conditions. The sensitivity of the telescope was 25 Jy/K.

From 1981 to 2005 a 128-channel filter-type analyzer with a resolution of 0.101 km/s was used. To obtain a sufficiently wide band (about 25 km/s) for a proper analysis of the emission features from the source under study, the observations were carried out in two stages, by adjusting the frequency of the first heterodyne of the receiver. Since 2005, a 2048-channel autocorrelation receiver with a resolution of 0.0822 km/s in radial velocity has been used. For S128 the range of overlapping in radial velocity was from −156 to 12 km/s.

To construct and analyze the figures we used only the central parts of the spectra where maser emission was observed (from −90 to −60 km/s). The uncertainty in the determination of the radial velocity was within 20-25 m/s. The intervals between two consecutive observations were of about one month. In 1993, 1994 and 2007, there were interruptions in the observations due to technical reasons. All spectra were adjusted for signal absorption in the Earth's atmosphere.

Whenever possible, the different S128 observations were carried out at positional angles close to each other. This made it possible to avoid noticeable changes in the angle between the polarization planes of the antenna feed and the source emission in the presence of linear polarization of the source maser emission.

In the program to compute the radial velocities, until March 2018, the velocity of the Sun's movement towards the apex was assumed to be 19.5 km/s. Since March 2018, we adopted a velocity value of 20 km/s. For this reason, the radial velocities of all spectra, as well as previously published observational results used in this paper, were corrected. The correction value for S128 was 0.36 km/s. Therefore, the total duration of the monitoring of the H_2O maser in S128 extends by more than 40 years. When constructing a 3D image, this observation period was divided into three intervals according to the following criteria: 1 – long duration of the entire monitoring; 2 – the different resolutions of the spectra in terms of radial velocity; 3 – the different structure of the spectra. Taking this into account, the following time intervals were chosen: 1981–2005, 2004.5–2006.0 and late 2005–early 2024. The time intervals overlap slightly in observation time.

Figures 3–5 show a three-dimensional (3D) representation of the evolution of H_2O maser emission in the S128 direction for all three observation intervals of our monitoring (1981-2024). Time in years, radial velocity in km/s and flux density in Jy are respectively represented in the x, y and z axes. This method requires a uniform series of data along the x and y axes. This condition was eventually but rarely not fulfilled on the time scale. In these time intervals, the spectra used in the 3D plots were obtained by triangulation of the fluxes of the original spectra, according to the times of the observations and of the regular times for the 3D plot. The obtained spectra were used to build the 3D plots.

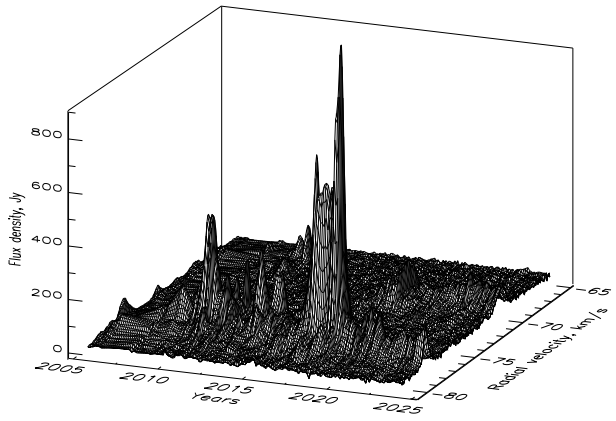

Fig. 5. 3D representation of H_2O spectra in S128 during the period 2005–2024 (see text).

For Figures 3 and 4, the observations have been made with a spectrum analyzer consisting of a bank of filters, and for Figure 5 with an autocorrelator. To construct a 3D image, the central part of the spectra was selected: from −80.0 to −68.5 km/s for Figure 3 and from −80.0 to −65.0 km/s for Figures 4 and 5, where maser emission H_2O was detected.

3. PROPERTIES OF H_2O MASERS A AND B

As we noted in the introduction, the H_2O maser emission in S128 was detected by Ho et al. (1981). They conducted observations of this maser in 1979 and 1980 at four epochs. The emission is concentrated mainly in the range of velocity from −88 to −65 km/s. In addition, two isolated features were observed at −89 and −57 km/s. According to Haschick & Ho (1985) and Migenes et al. (1999) the H_2O emission in S128 from −73 to −70 km/s belongs mainly to maser B, and the lower-velocity emission (< -76 km/s) comes mainly from source A.

As may be seen from Figures 3 to 5, during the entire time interval, the maser emission from both sources showed a flaring character. The flares were usually short-lived, which distinguishes the maser in S128 from masers in other sources, for example, from G43.8-0.1 (Colom et al. 2019). According to our long-term observations, in the time interval 2004-2006, the emission activity gradually shifted from maser B to maser A.

Two cycles of maser activity are identified. The first of them, from 1982 to 2004, is associated with maser B, and the second one, from 2006 to 2022, is associated with maser A. It should be noted that after 2022, the intensity of both masers dropped significantly.

It is important to note that prolonged, strong and rather variable maser emission was observed at radial velocities of −72 and −78 km/s for masers B and A, respectively. The nature of the emission of individual flares is more or less the same. The strongest flare with a flux density of 1700 Jy took place at −78.8 km/s in October 1985. The flare was short-lived and there was no significant increase in the emission intensity of the remaining features in the spectrum.

The second largest flare occurred 33 years later (in October 2018) at a similar velocity (−76.9 km/s) with a maximum flux density of 1320 Jy. It has been shown that this kind of flares can occur when at least two maser spots (Elitzur 1992), with close radial velocities, are randomly superimposed along the line of sight. In this case, an increase in the optical thickness of the ambient medium occurs and, consequently, a significant increase in the emission flux (see, for example, Lekht et al. (1983); Ashimbaeva et al. (2020)).

There are differences in the two activity cycles: the velocities of long-lived features vary significantly and the emission from source A is weaker than that from source B.

During the transition period between flare activity at sources B and A, which took place in 2004–2006, the shape of the H_2O spectrum clearly changed. The intensity of emission from both sources, during this period was approximately the same, as may be seen from Figure 4. It is possible to identify only one small flare at −75 km/s. Most likely, this detail belongs to the B source. It is known that the S128 source is at a distance from the Sun of 7.5 kpc; then, the linear distance between masers A and B is about $1.5 \cdot 10^{13}$ km. One may assume that the time interval between the end of the maser activity in A and the beginning of maser activity in B is of the order of 2 years. If the activity of the H_2O masers is associated with a disturbance propagating along the ionization front, then its velocity should be of the order of $2 \cdot 10^5$ km/s. Such a high value of the velocity is possible for the propagation not of the material itself, but of a perturbation of the ambient gas (its state, i.e. phase or areas of cloud contact). This may confirm the predominant role of cloud collisions in the generation of the H_2O maser emission.

The common cause of the variability of the maser emission of both masers may be shock waves occurring near the ionization front in the cloud contact region. The monitoring results suggest that such a region (disturbance) over time moves along the ionization front from south to north. At the same time, shock waves arise in such an area near the ionization

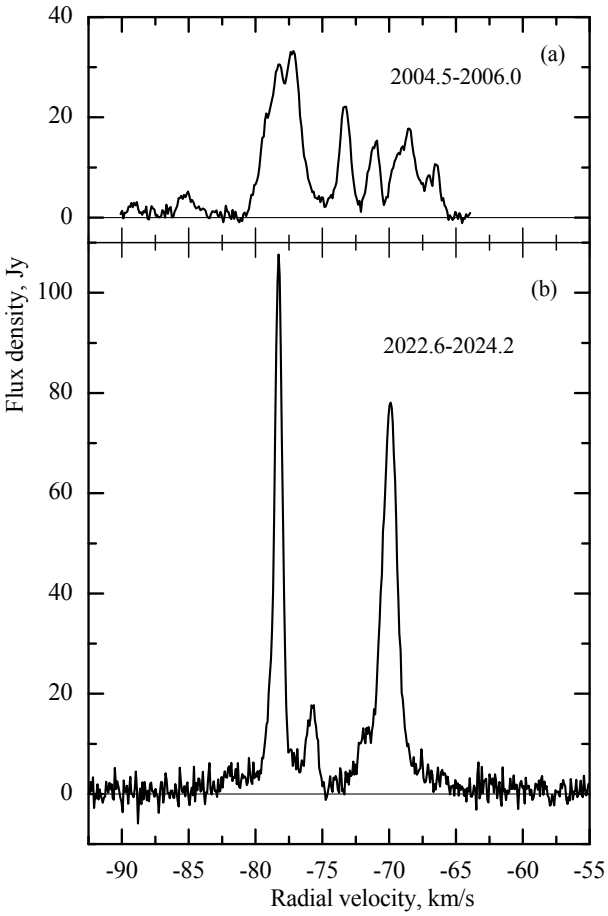

Fig. 6. The average spectra H_2O of two periods of minimal maser activity.

front, which stimulate the activity of maser condensations of sources B and A. This assumption confirms the results of Bohigas & Tapia (2003),that the star formation process in S128 proceeds in the south-north direction.

The activity of both masers (A and B) decreased significantly since the end of 2022. After that, there was a period of stable weak emission. Only the flux of two features, at −78.3 and −69.9 km/s, reached 140 and 100 Jy, respectively. The rest of the features were even weaker than the features during the transition period of 2003.5–2005.5. In addition, the emission disappeared at −89 km/s.

Figure 6 shows the average spectra of two periods of minimal maser activity. The stability of the emission during these periods allowed us to identify spectral features with a minimum flux density of up to 3 Jy. The radial velocities of the features in these two periods of low activity with a time difference of 20 years do not coincide, except for the detail at −78.3 km/s. The reason for the discrepancy could be the observed emission drift along the radial velocity (see, for example, Lekht et al. (2002); Ashimbaeva et al. (2018), which is a consequence of the impact of shock waves on maser condensations.

4. CONCLUSIONS

The main results of long-term observations of the H_2O maser emission in the direction of the S128 source, performed at the 22-m radio telescope in PRAO (Russia) in the period 1981–2024, are presented.

– The existence of a long-term evolution of the spectra, represented in a three-dimensional 3D image, is shown.

– It was found that in the time interval 2004–2006.0, the emission activity of H_2O gradually shifted from maser B to maser A.

– The duration of the active phase of the emission of masers B and A is about 23 and 16 years, respectively, i.e. quite close to each other.

– It was found that there are two periods of minimum activity of masers A and B in S128: 2004–2006 and after 2022.

– It is assumed that the common cause of the variability of maser emission from both sources (A and B) may be shock waves.They occur near the ionization front in the cloud contact region. Over time, this region (disturbance) shifts along the ionization front. According to the results of our monitoring, the disturbance is spreading in the south-north direction. This confirms the results of observations reported by Bohigas & Tapia (2003), that the star formation process occurs in the same direction.

It is assumed that the common cause of the variability of maser emission from both sources (A and B) may be shock waves occurring near the ionization front. At the same time, a disturbance propagates along such a front, which stimulates maser emission. According to the results of our monitoring, the disturbance is spreading in the south-north direction.

The authors are grateful to the staff of the Pushchino Radio Astronomy Observatory (Russia) for their substantial help in carrying out observations under the long-term monitoring program. The present study was conducted under the state assignment of Lomonosov Moscow State University.

REFERENCES

Ashimbaeva, N. T., Colom, P., Lekht, E. E., et al. 2018, ARep, 62, 609, https://doi.org/10.1134/S1063772918090019

Ashimbaeva, N. T., Krasnov, V. V., Lekht, E. E., et al. 2020, ARep, 64, 15, https://doi.org/10.1134/S1063772920010011
Ashimbaeva, N. T., Lekht, E. E., Krasnov, V. V., & Tolmachev, A. M. 2023, ARep, 67, 697, https://doi.org/10.1134/S1063772923070028
Berulis, I. I., Lekht, E. E., & Mendoza-Torres, J. E. 1995, ARep, 39, 411
Bohigas, J. & Tapia, M. 2003, AJ, 126, 1861, https://doi.org/10.1086/378054
Colom, P., Ashimbaeva, N. T., Lekht, E. E., et al. 2019, ARep., 63, 814, https://doi.org/10.1134/S0004629919100049
Elitzur, M. 1992, Astronomical masers, ASSL, 170, (Dorderecht, Kluwer), https://doi.org/10.1007/978-94-011-2394-5
Haschick, A. D. & Ho, P. T. P. 1985, ApJ, 292, 200, https://doi.org/10.1086/163147
Ho, P. T. P., Haschick, A. D., & Israel, F. P. 1981, ApJ, 243, 526, https://doi.org/10.1086/158617
Lekht, E. E., Likhachev, S. F., Sorochenko, R. L., & Strel'nitskii, V. S. 1983, ARep, 37, 367
Lekht, E. E., Mendoza-Torres, J. E., & Berulis, I. I. 2002, ARep, 46, 57, https://doi.org/10.1134/1.1436205
Mampaso, A., Gomez, P., Sanchez-Magro, C., & Selby, M. J. 1984, MNRAS, 207, 465, https://doi.org/10.1093/mnras/207.3.465
Migenes, V., Horiuchi, S., Slysh, V. I., et al. 1999, ApJ, 123, 487, https://doi.org/10.1086/313238
Richards, A. M. S., Cohen, R. J., Crocker, M., et al. 2005, ApSS, 295, 19, https://doi.org/10.1007/s10509-005-3652-7
Wood, D. O. S. & Churchwell, E. 1989, ApSC, 69, 831, https://doi.org/10.1086/191329
Wouterloot, J. G. A., Brand, J., & Henkel, C. 1988, AA, 191, 323

N. T. Ashimbaeva and V. V. Krasnov: Lebedev Physical Institute, Astro Space Center, Russian Academy of Sciences, Moscow, 117997 Russia.
E. E. Lekht: Lomonosov Moscow State University, Sternberg Astronomical Institute, Moscow, 119991 Russia (lekht@sai.msu.ru).
J. E. Mendoza-Torres: Instituto Nacional de Astrofísica, Óptica y Electrónica, Calle Luis enrique Erro No.1, Sta. María Tonantzintla, Puebla, CP 72840, México (mend@inaoep.mx).
V. R. Shoutenkov: Pushchino Radio Astronomy Observatory, Astro Space Center, Lebedev Physical Institute, Russian Academy of Sciences, Pushchino, 142290 Russia.